Chemistry and Physics of Lipids 224 (2019) 104794

Contents lists available at ScienceDirect

Chemistry and Physics of Lipids

journal homepage: www.elsevier.com/locate/chemphyslip

Optimization and characterization of rivastigmine nanolipid carrier loaded transdermal patches for the treatment of dementia

Meenakshi Kanwar Chauhan*, Pankaj Kumar Sharma

NDDS Research Laboratory, Department of Pharmaceutics, Delhi Institute of Pharmaceutical Sciences and Research, New Delhi, 110017, India

ARTICLE INFO

Keywords:
Rivastigmine
Transdermal patch
Nano lipid carriers

ABSTRACT

The present study aimed to develop nanolipid carrier (NLC) loaded transdermal system of rivastigmine for bioavailability enhancement. NLC was optimized using Box-Behnken Design (BBD). Optimized formulation comprises oil (4% w/w), tween 80 (3% w/w) and span 80 (1.8% w/w) and was characterized. It was found that the formulation exhibit 134.60 ± 15.10 nm, 0.286 ± 0.041, −11.80 ± 2.24 mV and 70.56 ± 1.20% of mean size, polydispersity index (PDI), zeta potential and entrapment efficiency, respectively. *In vitro* release studies showed there was more sustained release of drug from NLC loaded transdermal patches in comparison to Exelon® patch. Skin irritation studies proved the non-irritant nature of developed NLC based transdermal patch. From pharmacokinetic studies it was observed that there was increased C_{max} and AUC_{0-72} in plasma treated with NLC loaded transdermal patches as compared to conventional patch. These experimental results indicate that NLC based transdermal patch could be utilized as a potential carrier for enhancing bioavailability of rivastigmine for the better treatment and management of dementia.

1. Introduction

Nowadays, due to change in life styles, improper schedule, work stress and other contributed factors such as pollution, environmental free radicals as well as higher exposure of toxic chemicals, our current society is pooling into several neurological disorders and disease (Prince et al., 2015; Nigar et al., 2016). Among these neurological diseases, rapidly growing cases of dementia touched dangerous level of 45 million people and suffering population is estimated to be double in just next 20 years (Rao et al., 2014). Recently, it has drawn a lot of attention and concern from scientific community wherein they have addressed this world wide (49% of cases from Asia followed by 25% and 18%, from Europe and America, respectively) (Prince et al., 2015; Javed et al., 2017).

Acetylcholinesterases (AChE) and butrylcholinesterase (BuChE) enzymes inhibitors are used for management of dementia. These inhibitors lower the degradation of neuronal acetylcholine (ACh) thus maintain sufficient levels of Ach in the affected area of brain. However, donepezil and galantamine are also classified as cholinesterase inhibitors (ChEIs) but only rivastigmine has the ability to inhibit both AChE and BuChE. Studies indicates the clinical significance of rivastigmine in the clinical management of dementia over other drugs (Rao et al., 2014). Furthermore, as a matter of fact, cognitive impairment as well as adverse events like anorexia, vomiting and nausea in the quarter to half of the patients being treated with conventional oral dose regimen of rivastigmine at 6–12 mg/day; eventually lead to poor patient compliance and discontinuation of drug therapy (Kaduszkiewicz et al., 2005; Tiseo et al., 1998; Faulkner et al., 2005). To address these challenges in which compliance is impaired due to conventional dose related adverse effects or disease related dementia, novel formulations approaches and alternative route of administration with sustained release profile seem to be beneficial treatment strategies to be dependent upon.

In lieu of this, rivastigmine (9 mg) loaded daily replaceable Exelon transdermal patch® which releases up to 50% of the loaded drug *i.e.,* 4.5 mg from its 5 cm^2 of surface area over the period of 24 h, were commercially introduced for mild to moderate cases of Alzheimer's disease. But due to dose dumping and wastage of approximately 50% of the loaded drug from its patch as well as environmental consequences and economic burden on the patients; they are drawing a lot of concerns and debates too (Kurz et al., 2009; Lefèvre et al., 2008).

In this regard alternative to oral formulation, different nanotechnology approaches were adopted in last few decades and lipid based carrier systems emerged as most preferred in novel brain targeting drug delivery approach. Apart from favourable biocompatible profiles of lipid drug delivery systems; high rate to cross blood brain

* Corresponding author.
E-mail address: meenakshindds@gmail.com (M.K. Chauhan).

https://doi.org/10.1016/j.chemphyslip.2019.104794
Received 30 November 2018; Received in revised form 2 May 2019; Accepted 25 July 2019
Available online 27 July 2019
0009-3084/

barriers, controlled release of drugs, boosting the dissolution and solubilisation within the intestinal milieu and reduced gastric emptying rate with increase in mucosal permeability; further favours adaptation of these approaches and enhancement of poorly soluble drug bioavailability (Javed et al., 2018; Li et al., 2009; Suresh et al., 2007).

Of-late, among the lipid drug delivery system, solid lipid nanoparticles (SLNs) preferred as topical delivery system for BCS Class II drugs but due to some formulation limitation, such as low drug loading and drug leakage over the time due to solid lipid crystallization, NLCs have been introduced to overcome such issues, in order to achieve better therapeutic advantages. NLCs are the blend of solid lipid and oil which are stabilized by surfactant. NLCs are second generation and industrial applicable lipid nanoparticles in which integrated matrix of solid and liquid lipid favoring high drug loading and modulation of desired release profile of loaded drugs. In recent years, these systems are exploited to resolve the obstricles regarding topical delivery of lipophilic drugs. In these systems, the lipid core "hide" the hydrophobic drugs and the lipid matrix helps in transferring the drug across the biological membrane. Iqbal and associates suggested that NLCs are better in comparison to other lipid carrier systems in the dermal delivery of drug. These NLCs increases the skin hydration, increase drug movement through skin and reduce skin irritation (Muller et al., 2014; Iqbal et al., 2018). Hence, in transdermal drug delivery, these NLCs provide additional benefit owing to their occlusive property that enhances the penetration of drug by decreasing water loss from the skin as well as high permeation across the skin bilayer membranes (Doktorovova and Souto, 2009; Jenning et al., 2000; Wissing and Muller, 2002). Transdermal patches have various benefits compared to other routes of administration especially oral route. These systems are helpful in avoiding gastrointestinal and first pass metabolism of drug thus improving the bioavailability of those drugs which are susceptible to intestinal and first pass metabolism. It offers potential advantage of reduced doses of drug for an equal or better therapeutic effect and also the ability to interrupt treatment abruptly by removing the patch. This route helps in providing a desired plasma level compared with oral formulation. Transdermal delivery is a painless strategy hence improves patient compliance. Moreover, transdermal patches are non-invasive and can be self-administered. They can provide prolonged and steadier concentration of therapeutic moiety (Prausnitz and Langer, 2008; Pastore et al., 2015).

For the development of nanocarrier systems, there is need of controlling levels of excipients and the process parameters with the aim to achieve the good results. Thus, regulatory authorities like European Medicines Agency and FDA (USA) make use of quality by design (QbD) strategy to understand the process control QbD act as an effective technique in designing and formulation of different dosages. Moreover, response surface technique like BBD and central composite rotable design (CCRD) are widely employed in optimization of formulations. We employed BBD to factorial design to optimize rivastigmine loaded nanolipid carrier.

In present study, rivastigmine nanolipid carrier loaded transdermal patch (RV-NLCs patch) has been designed employing NLCs approach as compared with marketed transdermal Exelon® patch. In this respect, eudragit E-100 (EE-100) and poly-butyl methacrylate-co-methyl methacrylate (PBMACMA) were selected due to their stability and these have excellent fabrication property. Previously, these polymers were used in various formulation of transdermal delivery (Mutalik and Udupa, 2004; Mamatha et al., 2010). The encapsulation of drug in NLCs was done by using high pressure homogenization and optimized through three level three factor BBD (Agrawal et al., 2010; Alam et al., 2017). Further, the RV-NLCs patch were developed and evaluated for drug release, skin permeation and skin irritation studies in rats.

2. Materials and methods

2.1. Materials

Rivastigmine was procured as gift from Hetro Pharma (India). Castor oil was obtained from Loba Chemie Pvt Ltd, India. Capmul MCM was procured as a gift sample from Mohini Organics Pvt Ltd (India). Oils (soya oil, olive oil, palm oil and peanut oil) were purchased from Falcon, Bengaluru (India). Soy bean oil was purchased from Sigma-Aldrich, India. Tween 80 and span 80 were purchased from Merck, Mumbai, India. Eudragit E-100 was gifted by Evonik India Pvt. Ltd (India). Glyceryl monostearate was procured from CDH Ltd, India. Poly (butyl methacrylate-co-methyl methacrylate) (PBMACMA) polymer was purchased from Sigma Aldrich (USA). Polyvinyl pyrrolidone and diethyl phthalate were received from Loba Chemie (India). Exelon® patch (marketed rivastigmine transdermal patch) was procured from Novartis (India).

2.2. Methods

2.2.1. Screening of solid and liquid lipids

Solid lipid was chosen on the basis of drug solubility. Rivastigmine solubility in different lipids was estimated. The amount of drug and lipids was 10 mg and 500 mg, respectively. In case when drug was incapable to dissolve in lipid, further more lipid (100 mg) was used to dissolve the drug. Finally the mixtures were observed visually for drug solubility (Iqbal et al., 2018).

Liquid lipid (oil) was chosen on basis of maximum rivastigmine entrapment efficacy (Jitendra et al., 2013). In this connection, drug (100 mg) was weighed in centrifuge tubes containing 1gm of liquid lipids. The tubes were shaken for 24 h using water bath shaker at 37 ± 2 °C. Finally, the samples were centrifuged for twenty minutes at 5000 rpm and the amount of rivastigmine dissolved oil was determined by UV spectrophotometer at 214 nm.

2.2.2. Preparation and optimization of NLC

BBD was used in the study for optimization of NLCs. A three-level design was employed for exploring responses which were constructed with Design-Expert software (ver.9). Independent variables included ratio of solid and liquid lipid (X_1), ratio of tween 80 and span 80 (X_2) and number of HPH cycles (X_3). Other parameters, *i.e.,* amount of drug, homogenizer pressure, and final volume were kept constant. The dependent variables include particles size (Y_1), PDI (Y_2), zeta potential (Y_3) and encapsulation efficiency (Y_4) as given in Table 1. The levels for independent variables were selected on the basis of pre-formulation studies.

Rivastigmine loaded NLCs formulations were prepared by high pressure homogenization technique. Accurately weighed drug, solid lipid and liquid lipid were melted under continuous stirring at 70 ± 2 °C to form a transparent mixture. Separately, aqueous phase

Table 1
Variables with respective coded levels of BBD.

Factors Independent variables	Coded Levels		
	Low Level (-1)	Medium Level (0)	High Level (+1)
X_1 = Lipid: oil ratio	1	1.5	2
X_2 = Tween 80: Span 80 ratio	1.4	1.5	1.6
X_3 = HPH cycles	3	4	5
Dependent variables		Constrains	
Y_1 = Particle size		Minimum	
Y_2 = PDI		Minimum	
Y_3 = Zeta Potential		−25 to +25mV	
Y_4 = Entrapment efficiency		Maximum	

was prepared by dissolving 2% tween 80 in 10 ml of water. It was also maintained at a temperature of 70 ± 2 °C. Aqueous phase was gradually added to oil phase under continuous stirring at 2000 rpm using high speed homogenizer. This resulted mixture was subjected to high pressure homogenizer (GEA Niro Soavi Homogenizers Panda PLUS, Italy) to formulate NLCs at 500 bar using specific number of cycles. Obtained NLCs dispersion was cooled down on ice with gentle stirring for 10 min.

The following equation was produced for dependent variable.

$$Y_0 = b_0 + b_1X_1 + b_2X_2 + b_3X_3 + b_{12}X_1X_2 + b_{13}X_1X_3 + b_{23}X_2X_3 + b_{11}X_1^2 + b_{22}X_2^2 + b_{33}X_3^2$$

where, Y_0 is response variable; b_0 is intercept coefficient; b_1, b_2 and b_3 indicates linear coefficients; b_{11}, b_{22}, b_{33} are quadratic coefficients and b_{12}, b_{13}, b_{23} are interaction coefficients.

2.2.3. Characterization of NLCs

2.2.3.1. Particle size and PDI. NLCs particle size was measured in triplicate by Zetasizer (Malvern Instruments Ltd., UK). One milliliter sample were taken in cuvette and average particle size and PDI were measured at room temperature (24 ± 2 °C). Measurement was carried out by employing 90° of light scattering angle.

2.2.3.2. Surface charge determination. Zeta potential of rivastigmine-NLCs were estimated by Zetasizer (Malvern Instruments Ltd., UK). Estimation of zeta potential was done at temperature of 25 ± 2 °C and evaluation was performed in triplicate.

2.2.3.3. Attenuated total reflection (ATR). ATR was used for study of interaction between rivastigmine and excipients. ATR spectra of rivastigmine, excipients, physical mixture and rivastigmine loaded NLC were taken using an ATR spectroscopy instrument (Bruker, USA). ATR spectra over a spectral region from 4000 to 400 cm^{-1}. Chemical compatibility between excipients of NLC and drug were studied by comparing the obtained spectrums.

2.2.3.4. Thermal analysis. To assess interactions between drug and utilized lipid thermograms were constructed using differential scanning calorimetry (DSC, Universal V4.5A TA Instruments). The thermograms were recorded from a temperature range of 25 to 300 °C (Zhao et al., 2010). The heating rate was 10 °C/min.

2.2.3.5. Surface morphology study. Morphology of NLC was analysed by transmission electron microscopy (TEM). TEM was carried out by depositing a drop of NLC sample on wax paper. Sample was stained with phosphotungstic acid. Finally, after air drying the sample was analyzed for morphology with transmission electron microscope (PHILIPS TECHNAI-20, Japan), which was operated at 80 kV.

2.2.3.6. Entrapment efficiency. About one milligram of rivastigmine formulation was taken and mixed with methanol (10 ml). Then the mixture was centrifuged for 45 min at 15,000 rpm. The centrifugation was carried out at 4 °C by employing refrigerated centrifuge (Hettich Mikro 220R Centrifuge, UK). Supernatant was collected and amount of revastigmine was estimated by UV method. Percent entrapment efficiency was calculated by using given below equation

$$\text{Entrapment efficiency} = \frac{W_r - W_s}{W_r} \times 100$$

where, W_r = quantity of rivastigmine added in formulation

W_s = quantity of rivastigmine found in formulation

2.2.4. Incorporation of NLC in transdermal patch

Polymeric solution (20% w/v) was prepared by taking specified quantity (Table 2) of EE-100 and PBMACMA polymer with PVP 40 K, 5% (w/w) of di-butylpthalate, and 5% (w/w) of PEG 400 in a mixture of 2-propanol and dichloromethane (20:80 v/v) (Devi et al., 2003). Prepared solution (2 ml) was casted along with 1 ml of NLCs containing 30 mg of rivastigmine on circular glass mold (0.25 cm^2 area). The molds were placed at a temperature of 32 ± 2 °C in order to evaporate the solvent. After drying patches were packed in covers impermeable to moisture.

2.2.5. Characterization of transdermal patches

2.2.5.1. Thickness and weight variation. Thickness of NLCs integrated transdermal patch was measured by using a digital micrometer (Digital Caliper 150 mm, China) at random points on the patch. Measurements were taken by triplicate (Aggarwal et al., 2013).

2.2.5.2. Drug content estimation. A patch (weighing 100 mg) was dissolved in 10 ml mixture of 2-propanol and dichloromethane (20:80, v/v). The resulting mixture was shaken continuously for 24 h. Then solution was filtered and drug amount was determined UV spectrophotometer (at 214 nm) (Aggarwal et al., 2013).

2.2.5.3. Folding endurance. This parameter was estimated by folding the patch till it broke. Three patches of each type were taken for the test. The testing was carried out according to the procedure explained previously (Sarkar et al., 2014).

2.2.5.4. Surface pH. For this study phosphate buffer (10 ml) having pH 6.8 was taken in a beaker and patch was dispersed into it and pH of patch at the surface was measured at 1, 2, 3, 4, 5, 6, 7 and 8 h by the digital pH meter (Hanna Instrument, Mumbai). Experiments were performed in triplicate (Alam et al., 2009).

2.2.5.5. Moisture content. Patches were weighed individually. These were placed in desiccators at 27 ± 2 °C for 24 h. At regular time period, the patches were reweighed till a constant mass was achieved. Moisture content (%) was then estimated by using the given below formula (Mamatha et al., 2010).

$$\text{Moisture content } (\%) = \frac{\text{Initial weight of patch} - \text{Final weight of patch}}{\text{Final weight of patch}} \times 100$$

2.2.5.6. In-vitro drug release. Rivastigmine release experiment studies of NLCs integrated patches were carried out in a diffusion cell apparatus (Orchid Scientific, Nashik, India). A dialysis membrane-150 (Himedia, Mumbai) was utilized for estimating rivastigmine release. Twenty five milliliter of phosphate buffer (pH 7.4) was placed in receptor compartment. The media was stirred continuously and the temperature was maintained at 32 ± 0.5 °C (Sarkar et al., 2014). Samples (1 ml) were withdrawn at regular time periods upto 72 h. The same volume of fresh buffer was placed in receptor compartment. Rivastigmine concentration in samples was estimated by UV spectrophotometer at 214 nm.

2.2.5.7. Skin irritation test. This study was carried out on the basis of modified Draize test procedure (Sarkar et al., 2014). Albino Wistar rats (200–250 g) were used after approval of protocol by IAEC (IAEC/2016-I/06), DIPSAR, New Delhi (India). Hair at the dorsal abdominal skin of animals was shaved carefully. Animals were divided in two groups. First group was test drug group and second group was considered as standard irritant group. Transdermal patch was applied onto shaved skin of test drug group and covered with a micropore tape. Standard irritant group was applied with 0.8% v/v formalin solution. Patch was changed at every 24 h interval till the tested period of seven days. At the end of study period the score of erythema was recorded and was compared with standard. The score 0, 1, 2, 3 and 4 were given according to the severity of erythema (Draize et al., 1944). Absence of erythema scores 0. Presence of very slight erythema and well-defined

Table 2
Composition of transdermal patch of NLCs integrated transdermal patch.

Formulation code	Ratio of (EE-100 :PVP 40 K) (mg)	Ratio of (PBMACMA : PVP 40 K) (mg)	DBT (ml)	PEG-400	DCM:IPA (5:5) (ml)
F-1	8:2	–	0.1	0.125	10
F-2	6:4	–	0.1	0.125	10
F-3	4:6	–	0.1	0.125	10
F-4	–	8:2	0.1	0.125	10
F-5	–	6:4	0.1	0.125	10
F-6	–	4:6	0.1	0.125	10

erythema were indicated by a score of 1 and 2, respectively. For moderate type of erythema (indicated by light red colouration) a score of 3 was provided whereas severe erythema (indicated by presence of dark red colouration) a score of 4 was given.

2.2.5.8. Bioavailability studies

2.2.5.8.1. Assessment of rivastigmine loaded NLCs based transdermal patches pharmacokinetic parameters. Pharmacokinetic study was performed by using Albino Wistar rats (200–250 g) after approval of protocol by IAEC (IAEC/2016-I/06), DIPSAR, New Delhi (India). Animals were divided into three groups. In each group there were six rats. First and second groups were subjected to transdermal application of NLCs integrated PBMACMA patch and NLCs integrated EE-100 patch, respectively. Group third was animals subjected to transdermal application of marketed Exelon® patch. The area where patch was to be applied was shaved carefully and cleaned with warm water.

Blood samples were collected from tail vein and were centrifuged for 10 min at 4000 rpm. About 0.5 ml plasma was collected and mixed with 100 µl of tramadol (internal standard) working solution separately. Sample was vortexed for 10 min in a shaker. Ethyl acetate (3 ml) was added to the resultant sample and vortexed. Sample was kept on an ice bath for 5 min. The resultant mixture was then centrifuged at 8000 rpm for 10 min. Two milliliter of supernatant was collected and evaporated to dryness. The obtained material was reconstituted with methanol (500 µl) and vortexed for 10 s. A 20 µl sample was analyzed by HPLC for the estimation of rivastigmine.

2.2.5.8.2. Bioanalytical HPLC method. Samples of plasma were assayed for rivastigmine with a validated procedure using HPLC. HPLC system consisted of quaternary LC-10AT VP pump equipped with UV/VIS detector, SPD-10AVP column oven (Shimadzu), a Rheodyne injector and chromatography data system software (CLASS-VP Ver 6.14 SP1). Tramadol was used as internal standard. Chromatographic separation was carried out on HPLCrBEH C18 column (5 µm), Merck (Germany) with a mobile phase consisting of methanol:water (80:20, v/v) and a flow rate of 0.3 ml/min. Mobile phase was degassed prior to use. Samples (20 µl) were filtered (pore size, 0.45 µm) and injected by means of a Rheodyne injector and analyzed at 214 nm.

2.2.5.8.3. Pharmacokinetic analysis. Concentration rivastigmine-time profile in plasma after transdermal delivery was determined by software (PK Functions for Microsoft Excel, Pharsight Corporation, CA). Pharmacokinetic parameters (C_{max}, AUC_{0-6}: area under the curve between 0 and 6 h and $t_{1/2}$: half life) in plasma for different formulations were determined by using PK solution 2.0 software for each group.

3. Results and discussion

3.1. Screening of liquid and solid lipids

Drug solubility in lipids is an important determinant factor for the entrapment and successful formulation of NLCs. Solubility of rivastigmine was assessed in liquid and solid lipids. Solubility of rivastigmine in various lipids is listed in Table 3. Among the tested solid lipids, rivastigmine exhibit highest solubility in glycerol monostearate (1.843 ± 0.231 mg/gm) and was selected for further processing. The solubility was evaluated in liquid lipid; it showed maximum solubility in castor oil which amounted up to 24.37 ± 0.40 mg/ml. Besides acting as a solubilizing lipid for rivastigmine, castor oil is also known to increase the transdermal penetration of drugs (Johnson, 2007). This characteristic feature of it might had a significant impact on the penetration of rivastigmine through the skin.

Table 3
Solubility of rivastigmine in various solid lipids (S) and liquid lipids (L).

Lipids	Rivastigmine solubility
Glycerylmonooleate (S)	0.231 ± 0.014 mg/gm
Glycerylmonosterate (S)	1.843 ± 0.231 mg/gm
Stearic acid (S)	0.307 ± 0.025 mg/gm
Oleic acid (S)	0.165 ± 0.011 mg/gm
Capmul MCM C8 (S)	18.41 ± 0.20 mg/ml
Castor oil (L)	24.37 ± 0.40 mg/ml
Soya oil (L)	22.49 ± 0.62 mg/ml
Soyabean (L)	4.093 ± 0.48 mg/ml
Olive oil (L)	14.47 ± 0.45 mg/ml
Palm oil (L)	14.61 ± 0.72 mg/ml
Peanut oil (L)	17.87 ± 0.48 mg/ml
Squalene (L)	4.86 ± 0.15 mg/ml

3.2. Optimization of NLC

Design expert software generated 17 batches. Table 4 listed the different variables and the achieved responses. Different equations were also produced to estimate the influence of independent variables on formulation characteristics. The positive symbol demonstrates increased influence on the dependent variable and the negative symbol demonstrate decreased effect on dependent variables (Alam et al.,

Table 4
Formulation composition and the effect on different formulation variables on particle size (Y_1), polydispersity index (Y_2), zeta potential (Y_3) and entrapment efficiency (Y_4).

Samples	Factors			Responses			
	X_1	X_2	X_3	Y_1(nm)	Y_2	Y_3 (mV)	Y_4 (%)
F1	1	1.4	4	155.02	0.466	−11.46	68.90
F2	1.5	1.5	4	187.45	0.401	−15.10	69.02
F3	1.5	1.6	5	181.31	0.301	−13.70	66.43
F4	2	1.6	4	197.00	0.315	−12.40	80.30
F5	1	1.6	4	130.35	0.320	−12.30	66.80
F6	1.5	1.5	4	184.08	0.398	−14.90	68.20
F7	1.5	1.4	5	189.10	0.468	−14.10	70.07
F8	2	1.5	5	192.43	0.419	−12.90	79.21
F9	1.5	1.5	4	182.04	0.397	−14.30	67.00
F10	2	1.4	4	190.18	0.456	−13.60	81.92
F11	2	1.5	3	198.70	0.324	−13.10	82.09
F12	1.5	1.6	3	182.00	0.304	−13.70	69.90
F13	1	1.5	5	152.06	0.406	−11.90	65.00
F14	1.5	1.5	4	182.23	0.394	−15.70	69.80
F15	1.5	1.4	3	185.05	0.423	−14.50	70.42
F16	1.5	1.5	4	185.52	0.366	−15.00	68.10
F17	1	1.5	3	149.00	0.315	−12.30	71.41

Table 5
Summary of results of regression analysis for responses.

Response	Model	R^2	Adjusted R^2	Predicted R^2	Standard deviation (%)	Mean
Y_1	Quadratic	0.991	0.980	0.908	2.67	177.65
Y_2	Linear	0.887	0.860	0.788	0.02	0.38
Y_3	Quadratic	0.955	0.897	0.861	0.40	−13.59
Y_4	Quadratic	0.982	0.959	0.842	1.14	71.32

2017). From Table 5 data it was suggested that the difference in correlation coefficient (R^2) was less than 1 indicating good fit of model. Moreover, the difference of less than 0.2 between the 'adjusted R-squared' and 'predicted R-squared' indicated good value agreement. Fig. 1 demonstrate three-dimensional plots which explain the influence of formulation constituents on the dependent variables.

3.3. Characterization of optimized NLC

3.3.1. Particle size and particle size distribution (PDI)

Particle size of optimized rivastigmine NLCs was as found to be 134.60 ± 15.10 nm (Fig. 2a). Small size ensured better permeation due to increased surface area resulting in more quantity of rivastigmine being transported across the skin resulting in increased therapeutic effect at minimized frequency of dosing. PDI value of 0.286 ± 0.041 was found for optimized formulation indicating narrow size distribution as well as particle size uniformity of formulation.

3.3.2. Surface charge determination

Zeta potential influences NLCs stability because it suggests the attraction or repulsion between particles. NLC charge was found to be -11.80 ± 2.24 mV suggesting production of stable formulation (Fig. 2b). The negative charge of nanoparticles could be due to the presence of free fatty acids of the liquid and solid lipids used in formulation of NLCs.

3.3.3. ATR

ATR study was carried out to find out any possible interaction taking place between rivastigmine and excipients in NLC preparation. Spectra of rivastigmine, castor oil, glyceryl monostearate, physical mixture (drug, castor oil and glyceryl monostearate) and optimized drug loaded NLC are shown in Fig. 3. The different characteristic peaks of drug, excipients and formulation are listed in Table 6. The ATR spectra of rivastigmine showed characteristic absorption peaks, C–H (stretching), NHCO (stretching), C–N (stretching) and C–O (stretching) vibrations. It was observed that all major peaks in ATR of pure drug were retained in physical mixture of drug, glyceryl monostearate and castor oil suggesting that there was no interaction between rivastigmine and excipients (Fig. 3). Physical mixture showed characteristic peaks of drug and excipients corresponding to C–H, C═O, C–N, C–O and C–H (bending) functional groups. Thus, in physical mixture the vibration

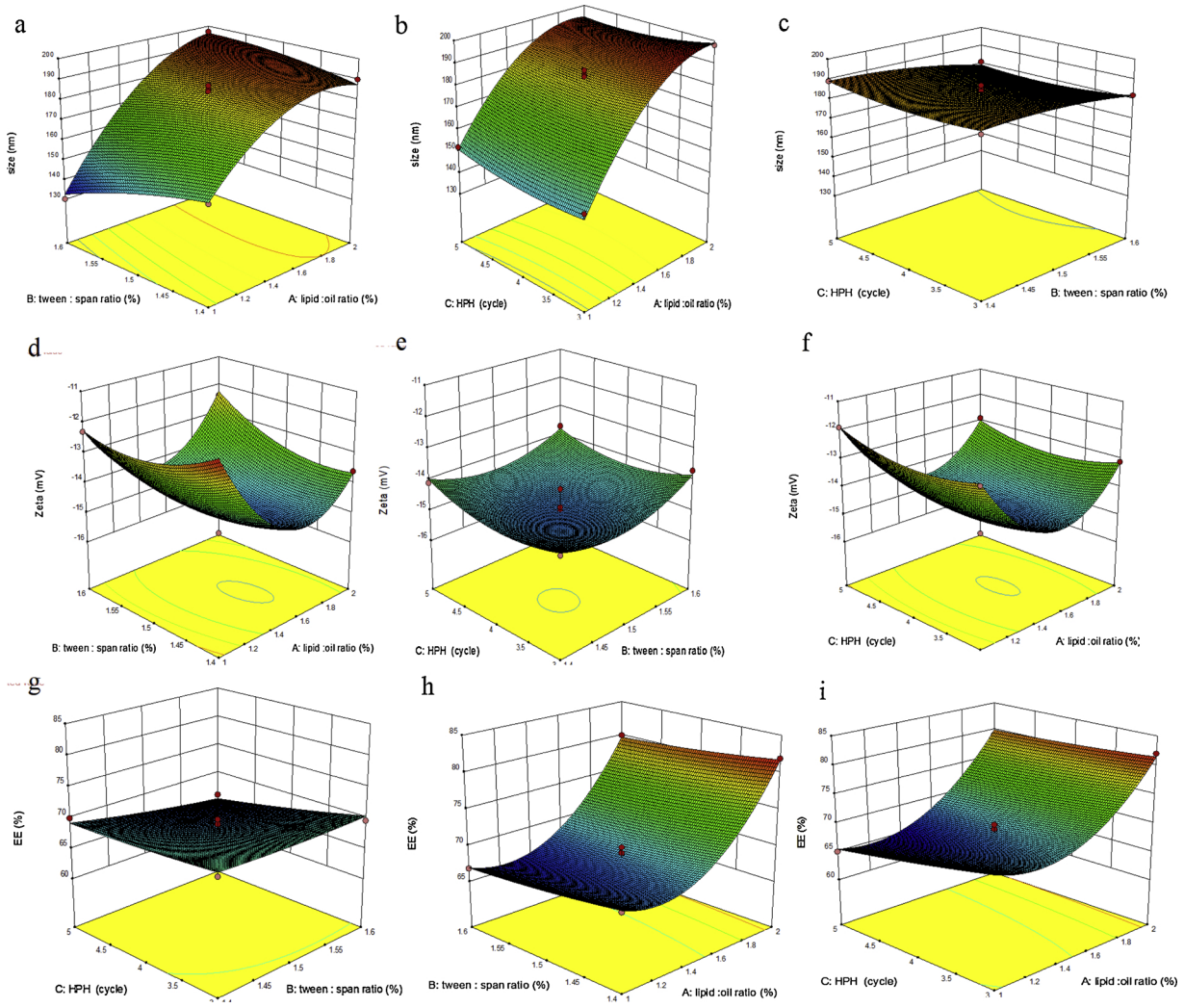

Fig. 1. Response surface plots showing effect of independent variables on particle size (a–c), zeta potential (d–f) and entrapment efficiency (g–i).

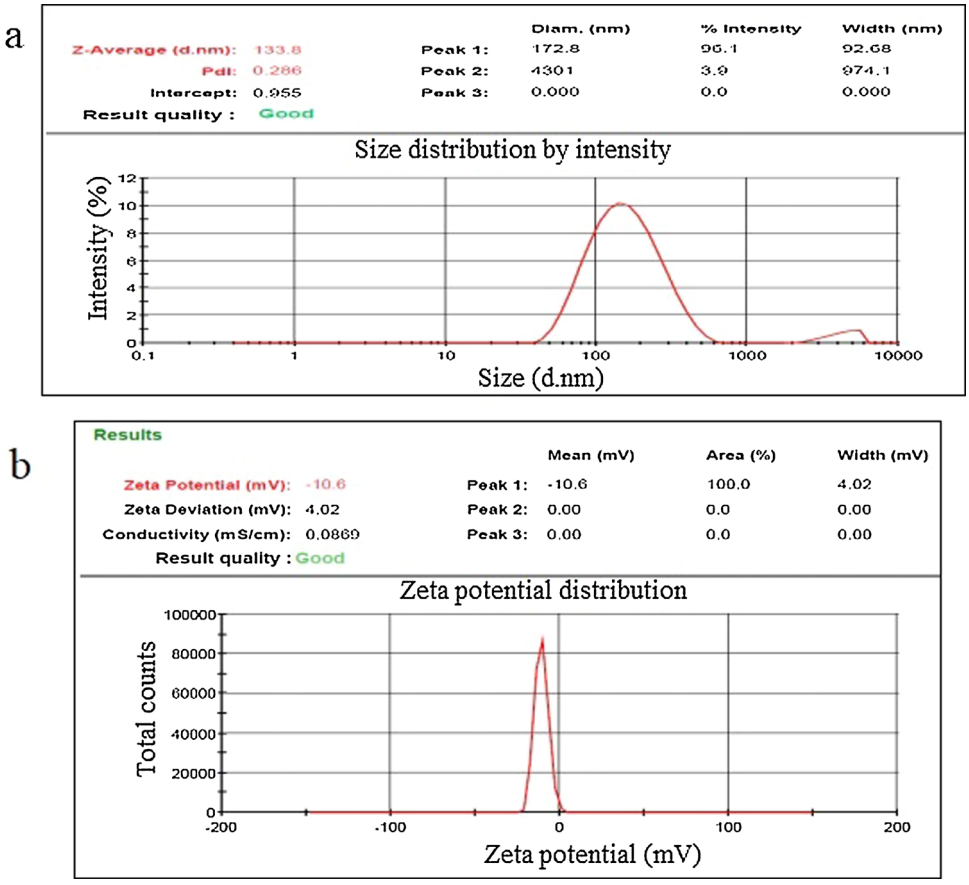

Fig. 2. (a) Particle size and size distribution (PDI) of optimized NLC; (b) zeta potential of optimized NLC.

bands were not affected by the excipients of NLC as the entire drug peaks were present in the physical mixture which showed intactness of drug in mixture and absence of any possible interaction between drug and formulation ingredients. The main characteristic peak of carbamates (−CONH) group in rivastigmine structure exhibit less intensity in rivastigmine loaded-NLCs, suggesting encapsulation of drug in nanolipid carrier (Yuxiu et al., 2014). Moreover, in rivastigmine loaded NLC the vibration bands were not affected by the excipients of NLC as the entire drug peaks were present in the NLC which showed intactness of drug in formulation and absence of any possible interaction between drug and formulation ingredients.

3.3.4. Thermal analysis

DSC thermograms for pure drug, physical mixture and patterns of lyophilized rivastigmine loaded NLC are shown in Fig. 4. DSC is usually used to provide information on physical properties of a compound or formulation, by measuring the heat loss or gain resulting from physical or chemical changes within a sample as a function of the temperature. DSC also gives an insight into the melting and re-crystallization behavior of crystalline materials. Rivastigmine, physical mixture and rivastigmine loaded NLC were subjected the DSC to assess a possible melting point depression of the lipid and thermal behavior of the materials. The results are shown as DSC thermograms in Fig. 4. The melting point depression of drug can be seen when the drug is in the mixture. Fang et al. reported that the solubilization of drug in lipid matrix could be enhanced when the sample was heated up (Fang et al., 2008). In the present study, DSC thermograms of drug-loaded NLC demonstrate no melting peak of revastigmine. It is considered that the drug was already dissolved in the melting lipid phase during the nanocarriers preparation. This result is in good accordance with the previously reported by Okonogi and Riangjanapatee when lycopene is being molecularly dispersed in the lipid matrix (Okonogi and Riangjanapatee, 2014).

3.3.5. Surface morphology study

Morphology of nanoparticles were analysed by TEM. It was found that the optimized NLC had uniform, spherical and sub-spherical in shape particles and there was no particle aggregation (Fig. 5a).

3.3.6. Entrapment efficiency

Percentage of incorporated rivastigmine in lipid matrix (entrapment efficiency) was determined. Entrapment efficiencies of formulations was found to be 70.56 ± 1.20%. Incorporation of rivastigmine results in high entrapment efficiency due to its lipophilic nature.

3.4. Evaluation of patch

3.4.1. Physical parameters of patch

Prepared RV-NLCs patches were uniform, transparent and smooth. The different evaluated parameters for patches are listed in Table 7. Determined weight of patches was found in range of 418.04 ± 3.09 mg to 505.10 ± 3.65 mg which indicated that patch weights of various batches were relatively similar. There was also similarity between the patches thickness. From these results it was suggested that there is reproducibility of patches.

3.4.2. Drug content

Fabricated RV-NLCs patches exhibit comparable drug concentration. Concentration of rivastigmine in patches were ranged from 96.20 to 99.70% (Fig. 5b).

3.4.3. Moisture uptake

Patches developed in our laboratory showed

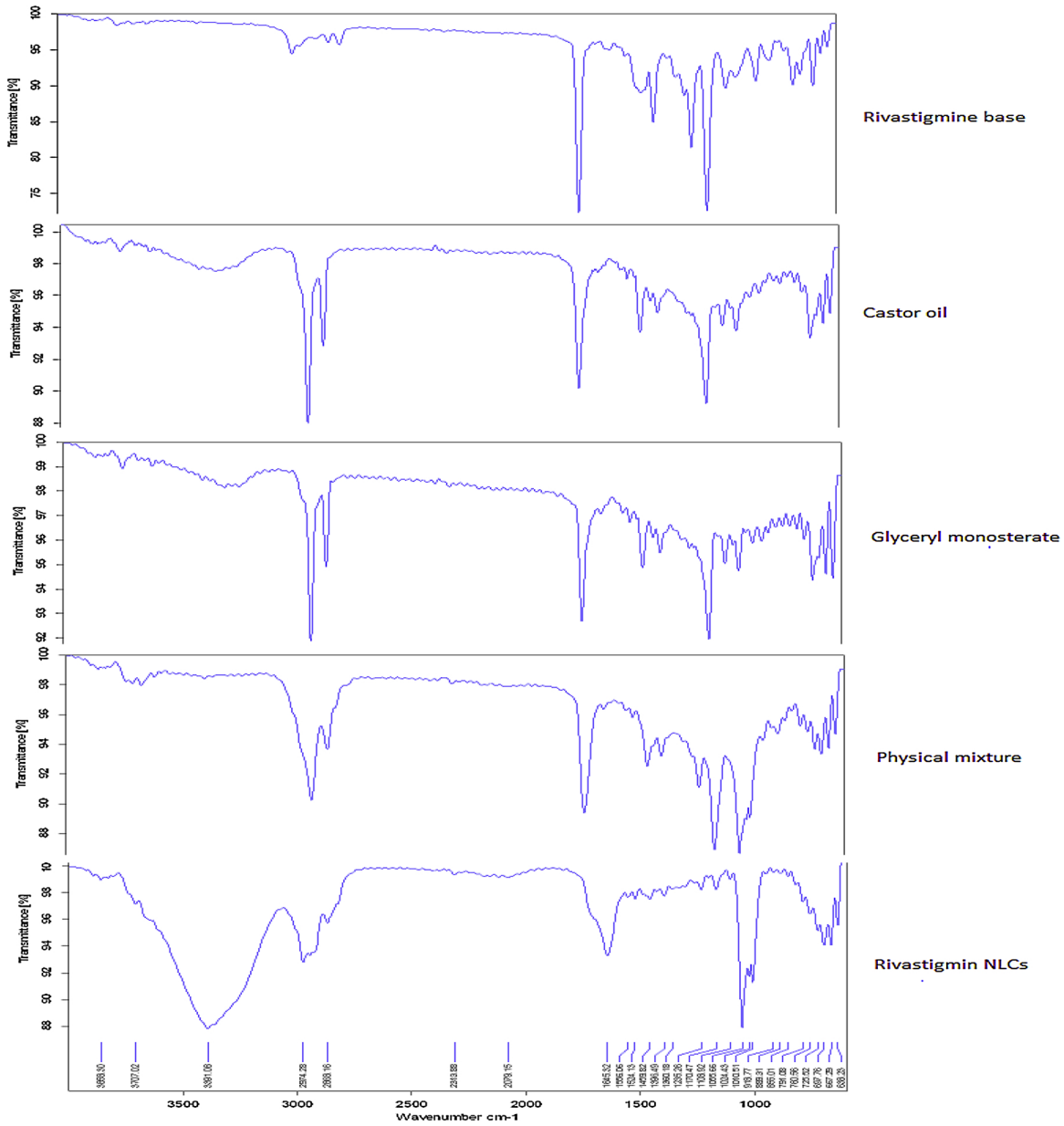

Fig. 3. ATR spectra of rivastigmine, castor oil, glyceryl monostearate, physical mixture (drug, castor oil and glyceryl monostearate) and optimized drug loaded NLC.

Table 6
Interpretation of ATR spectra for drug incompatibility.

Materials	Characteristics peaks
Rivastigmine	2976.06, 2818.31, 2769.08 C-H (stretching);1772.31 (NHCO, carbamates) (stretching); 1161.97 C-N (stretching) and 1231.02 C-O (stretching)
Castor oil	2917.44 C-H (stretching); 1734.21 (C = O) (stretching) and 1651.97 C = C (stretching)
Glyceryl monostearate	3612.13 O-H (stretching); 2916.96, 2850.39 C-H (stretching); 1650.92 (C = O) (stretching) and 1018.42 C-H (bending)
Physical mixture	2976.41, 2828.05 C-H (stretching); 1732.52 C = O (stretching); 1160.52 C-N (stretching) and 1233.11 C-O (stretching) and 1017.47 C-H (bending)
Rivastigmine-loaded NLCs	3391.08 O-H (stretching); 2974.28, 2868.16 C-H (stretching); 1645.32 (C = O) (stretching) and 1010.51 C-H (bending)

0.747 ± 0.020%–4.024 ± 0.030% moisture absorption indicating stable and microbial growth resistant patches. Patches made with different polymer were found to have significant ($p < 0.05$) moisture absorption differences. As PVP-K30 concentration increased the moisture absorption capacity was found to be increased as shown in Table 7.

3.4.4. In-vitro release of NLCs integrated transdermal patch system

3.4.4.1. Using EE-100 matrix and PBMACMM matrix of patch. *In-vitro* release profile of marketed Exelon patch® (4.6 mg/24 h) showed faster release rate than optimized RV-NLCs integrated EE-100 and PBMACMA acrylate polymer matrix (Fig. 5c). Drug release profile from the two patches (EE-100 and PBMACMA patch matrix) was almost identical. Drug release profile of rivastigmine from lipid carrier indicated the sustained release of drug, clearly indicating in entrapment of drug into

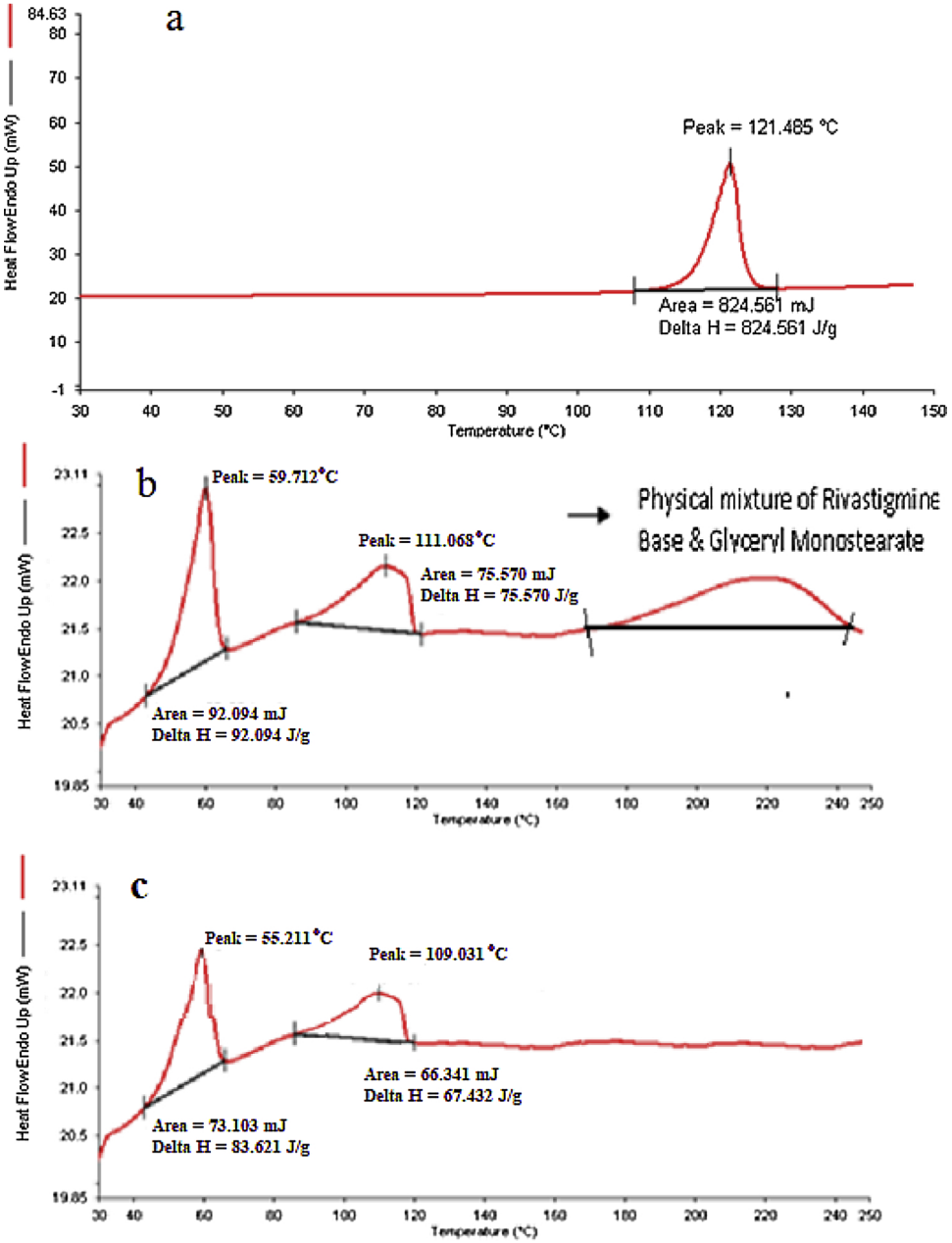

Fig. 4. DSC thermogram pattern of (a) pure rivastigmine, (b) physical mixture and (c) rivastigmine loaded NLC.

lipid matrix and solid core made up of glyceryl monostearate might be responsible for the slow release effect (Bhaskar et al., 2008; Tiwari and Pathak, 2011). *In-vitro* studies showed that the percentage cumulative release of marketed Exelon® patch (4.5 mg/24 h) was 95.68 ± 0.21% in 24 h and optimized RV-NLCs integrated EE-100 and PBMACMA acrylate patch were 98.12 ± 0.11% and 96.85 ± 1.12% after 72 h, respectively.

3.5. Skin irritation study

After application of RV-NLCs loaded patches on rat skin it was observed visually for any sign of irritation. There was no sign of irritation which showed that the developed patch exhibit non-irritant nature. Hence, these developed formulations are safe.

3.6. Pharmacokinetic test of the studied transdermal patches in rats

Pharmacokinetic parameter (listed in Table 8) of optimised revastigmine-NLCs patches and Exelon® patch in rat plasma after transdermal application were determined. It could be seen that the maximum drug concentration in plasma appeared 16.94 ± 0.58 µg/ml, 16.87 ± 0.62 µg/ml and 16.92 ± 0.31 µg/ml for PBMACMA patch, EE-100 patch and Exelon® patch, after topical application, respectively. AUC for NLCs integrated transdermal patches were found to be 865.70 ± 5.88 µg/ml/h and 823.87 ± 5.52 µg/ml/h for PBMACMA patch and EE-100 patch, respectively and were 1.5-fold higher compared to Exelon® patch (AUC was 552.17 ± 3.65 µg/ml/h) as shown in Fig. 5d. Approximately similar C_{max}, extended T_{max} and higher AUC of RV-NLCs integrated transdermal patch in rats showed that the release of drug from NLCs imbedded patch is slow and thus provide a prolonged as well as sustained action of the drug (Fazil et al., 2012).

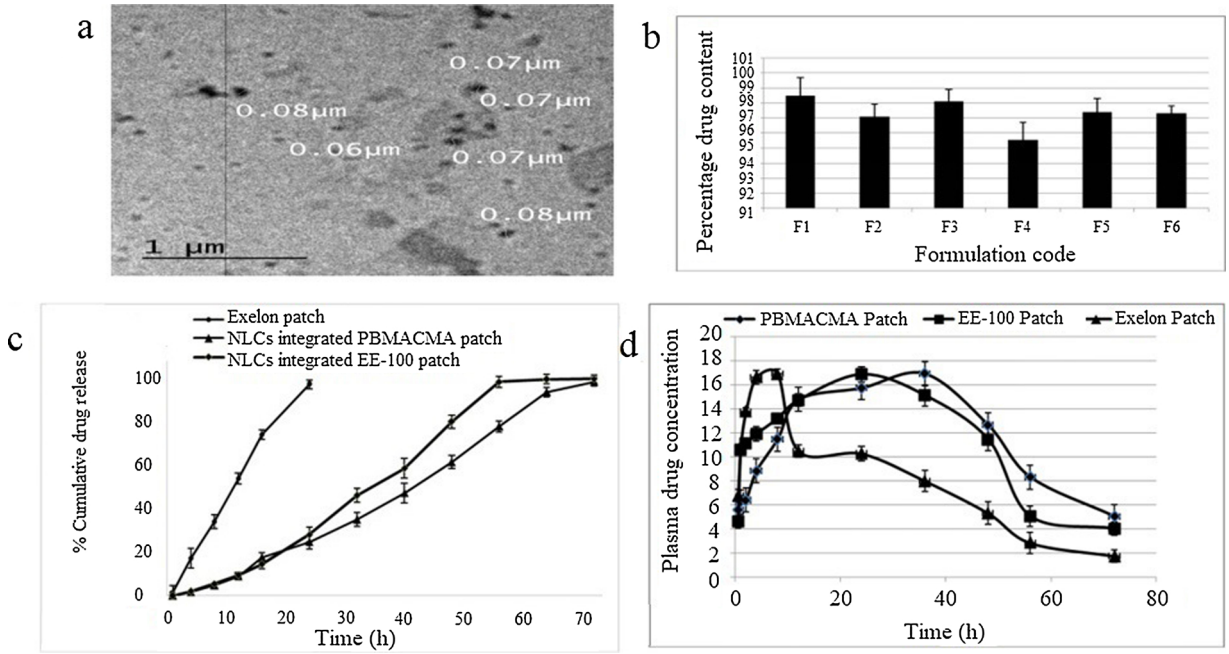

Fig. 5. (a) TEM of drug loaded NLC; (b) percentage drug content of different transdermal patch formulations; (c) drug release pattern of NLCs integrated transdermal patch and marketed Exelon® patch; and (d) plasma drug concentration profile of transdermal patch after topical application to rats.

Table 7
Physical characterization data for the transdermal patches.

Formulation	Weight (mg) ± SD	Thickness (mm) ± SD	Folding endurance ± SD	Flatness	Diameter (cm) ± SD	Area (cm^2) ± SD	Surface pH ± SD	Moisture uptake (%) ± SD
F-1	437.02 ± 2.34	0.65 ± 0.01	680.03 ± 4.56	100.00	2.58 ± 0.05	8.10 ± 0.28	5.67 ± 0.34	0.74 ± 0.07
F-2	497.21 ± 3.21	0.61 ± 0.02	695.41 ± 5.23	100.00	2.55 ± 0.01	8.01 ± 0.15	5.48 ± 0.24	2.01 ± 0.06
F-3	505.10 ± 3.65	0.60 ± 0.02	675.01 ± 5.63	100.00	2.59 ± 0.22	8.13 ± 0.42	5.51 ± 0.37	4.02 ± 0.14
F-4	430.51 ± 5.01	0.55 ± 0.01	710.11 ± 5.08	100.00	2.58 ± 0.02	8.10 ± 0.51	5.68 ± 0.36	0.83 ± 0.44
F-5	418.04 ± 3.09	0.58 ± 0.01	680.00 ± 6.23	100.00	2.57 ± 0.14	8.07 ± 0.33	5.62 ± 0.34	2.24 ± 0.74
F-6	467 ± 3.24	0.64 ± 0.02	667.45 ± 5.11	100.00	2.61 ± 0.03	8.17 ± 0.56	5.70 ± 0.42	3.50 ± 0.78

Table 8
Pharmacokinetics parameters of transdermal patch in rat plasma.

Parameters	PBMACMA patch	EE-100 patch	Exelon®patch
C_{max} (μg/ml)	16.94 ± 0.58	16.87 ± 0.62	16.92 ± 0.31
T_{max} (h)	36.10 ± 0.25	24.14 ± 0.18	8.03 ± 0.11
Ke (h^{-1})	4.24 ± 0.12	1.84 ± 0.11	0.43 ± 0.02
AUC_{0-72} (μg/ml/h)	865.70 ± 5.88	823.87 ± 5.52	552.17 ± 3.65

4. Conclusion

In this study a RV-NLCs loaded patch was developed by using castor oil and glyceryl monosterate. *in vitro* studies showed that formulation exhibit good therapeutic efficacy. It was concluded from animal studies that RV-NLCs loaded patches showed more bioavailability in comparison to conventional dosage. The present work has shown good outcomes thus there is feasibility of fabricating rivastigmine transdermal patch. The developed RV-NLCs based patch may confirm to be a good alternative to conventional formulations and could be utilized in the management of dementia.

Declaration of Competing Interest

The author report no conflict of interest.

Acknowledgments

The authors are sincerely thankful for financial support provided by Department of Science and Technology, (New Delhi), to carry out the research work under Project No. SB/YS/LS-41/2011.

References

Aggarwal, G., Dhawan, S., Hari Kumar, S.L., 2013. Formulation, in vitro and in vivo evaluation of transdermal patches containing risperidone. Drug Dev. Ind. Pharm. 39 (1), 39–50.
Agrawal, Y., Petkar, K.C., Sawant, K.K., 2010. Development, evaluation and clinical studies of acitretin loaded nanostructured lipid carriers for topical treatment of psoriasis. Int. J. Pharm. 401, 93–102.
Alam, M.I., Baboota, S., Kohli, K., Ali, J., Ahuja, A., 2009. Development and evaluation of transdermal patches of celecoxib. PDA J. Pharm. Sci. Technol. 63, 429–437.
Alam, M.S., Garg, A., Saifullah, M.K., Tareq, A.I., Mohsin, M., Manzoor, O., Pottoo, F.H., Javed, M.N., 2017. Gum ghatti mediated, one pot green synthesis of optimized gold nanoparticles: investigation of process-variables impact using Box-Behnken based statistical design. Int. J. Biol. Macromol. 104 (A), 758–767.
Bhaskar, K., Krishna, M., Lingam, M., Prabshakar, R., Venkateswardu, V., Madhusudan, R., 2008. Development of nitrendipine controlled release formulations based on SLN and NLC for topical delivery: in vitro and ex vivo characterization. Drug Dev. Ind. Pharm. 34, 719–725.
Devi, V.K., Saisivam, S., Maria, G.R., Deepti, P.U., 2003. Design and evaluation of matrix diffusion controlled transdermal patches of verapamil hydrochloride. Drug Dev. Ind. Pharm. 29, 495–503.
Doktorovova, S., Souto, E.B., 2009. Nanostructured lipid carrier-based hydrogel formulations for drug delivery: a comprehensive review. Expert Opin. Drug Deliv. 6, 165–176.
Draize, J.H., Woodard, G., Calvery, H.O., 1944. Methods for the study of irritation and toxicity of substances applied topically to the skin and mucous membranes. J. Pharmacol. Exp. Ther. 82, 377–390.

Fang, J.Y., Fang, C.L., Liu, C.H., Su, Y.H., 2008. Lipid nanoparticles as vehicles for topical psoralen delivery: solid lipid nanoparticles (SLN) versus nanostructured lipid carriers (NLC). Eur. J. Pharm. Biol. 70, 633–640.

Faulkner, J.D., Bartlett, J., Hicks, P., Di Piro, J.T., Talbert, R.L., Yee, G.C., Matzke, G.R., Wells, B.G., Posey, L.M., 2005. Alzheimer's Disease: Pharmacotherapy—A Pathophysiologic Approach, MCGRAW-HILL Medical Publishing Division, USA. pp. 1157–1174.

Fazil, M., Haque, M.S., Kumar, M., Baboota, S., Sahni, J.K., Ali, J., 2012. Development and evaluation of rivastigmine loaded chitosan nanoparticles for brain targeting. Eu. J. Pharm. Sci. 47, 6–15.

Iqbal, B., Ali, J., Baboota, S., 2018. Silymarin loaded nanostructured lipid carrier: from design and dermatokinetic study to mechanistic analysis of epidermal drug deposition enhancement. J. Mol. Liq. 255, 513–529.

Javed, M.N., Alam, M.S., Pottoo, F.H., 2017. Metallic nanoparticle alone and/or in combination as novel agent for the treatment of uncontrolled electric conductance related disorders and/or seizure, epilepsy & convulsions. PCT Pat. Appl WO2017060916 A1.

Javed, M.N., Kohli, K., Amin, S., 2018. Risk assessment integrated QbD approach for development of optimized bicontinuous mucoadhesive limicubes for oral delivery of Rosuvastatin. AAPS Pharm. Sci. Tech. 31 (January), 1–5.

Jenning, V., Thünemann, F., Gohla, S.H., 2000. Characterisation of a novel solid lipid nanoparticle carrier system based on binary mixtures of liquid and solid lipids. Int. J. Pharm. 199, 167–177.

Jitendra, K., Ashwin, K.P., Raj, K., Kanwar, C.M., 2013. Formulation, characterization and in vitro–in vivo evaluation of flurbiprofen-loaded nanostructured lipid carriers for transdermal delivery. Drug Dev. Ind. Pharm. 39, 569–578.

Johnson, W., 2007. Final report on the safety assessment of *Ricinus communis* (castor) seed oil, hydrogenated castor oil, glyceryl ricinoleate, glyceryl ricinoleate SE, ricinoleic acid, potassium ricinoleate, sodium ricinoleate, zinc ricinoleate, cetyl ricinoleate, ethyl ricinoleate, glycol ricinoleate, isopropyl ricin. Int. J. Toxicol. 26, 31–77.

Kaduszkiewicz, H., Zimmermann, T., Beck-Bornholdt, H.P., Bussche, H.V., 2005. Cholinesterase inhibitors for patients with Alzheimer's disease: systematic review of randomised clinical trials. BMJ 331, 321–327.

Kurz, A., Farlow, M., Lefèvre, G., 2009. Pharmacokinetics of a novel transdermal rivastigmine patch for the treatment of Alzheimer's disease: a review. Int. J. Clin. Pract. 63, 799–805.

Lefèvre, G., Sędek, G., Jhee, S.S., Leibowitz, M.T., Huang, H.L., Enz, A., Maton, S., Ereshefsky, L., Pommier, F., Schmidli, H., Appel Dingemanse, S., 2008. Pharmacokinetics and pharmacodynamics of the novel daily rivastigmine transdermal patch compared with twice-daily capsules in Alzheimer's disease patients. Clin. Pharmacol. Ther. 83, 106–114.

Li, H., Zhao, X., Ma, Y., Zhai, G., Li, L., Lou, H., 2009. Enhancement of gastrointestinal absorption of quercitin by solid lipid nanoparticles. J. Control Release 133, 238–244.

Mamatha, T., Venkateswara Rao, J., Mukkanti, K., Ramesh, G., 2010. Development of matrix type transdermal patches of lercanidipine hydrochloride: physicochemical and in-vitro characterization. DARU 18, 09–16.

R.H. Muller, A. Lippacher, S. Gohla, Solid–liquid (semi-solid) lipid particles and method of producing highly concentrated lipid particle dispersions, U.S.A Pat Appl. US8663692 B1 8 (2014) 663-692.

Mutalik, S., Udupa, N., 2004. Glibenclamide transdermal patches: physicochemical, pharmacodynamic, and pharmacokinetic evaluations. J. Pharm. Sci. 93, 1577–1594.

Nigar, S., Pottoo, F.H., Tabassum, N., Verma, S.K., Javed, M.N., 2016. Molecular insights into the role of inflammation and oxidative stress in epilepsy. JOAMPS 10, 1–9.

Okonogi, S., Riangjanapatee, P., 2014. Potential technique for tiny crystalline detection in lycopene-loaded SLN and NLC development. Drug Dev. Ind. Pharm. 40, 1378–1385.

Pastore, M.N., Kalia, Y.N., Horstmann, M., Roberts, M.S., 2015. Transdermal patches: history, development and pharmacology. Br. J. Pharmacol. 172, 2179–2209.

Prausnitz, M.R., Langer, R., 2008. Transdermal drug delivery. Nat. Biotechnol. 26, 1261–1268.

Prince, M., Wimo, A., Guerchet, A., Gemma-Claire, A., Wu, Y.T., Prina, M., 2015. World Alzheimer report: the global impact of dementia, an analysis of prevalence, incidence, cost and trends. Alzheimer's Dis. Int. 84, 01–92.

Rao, A.T., Degnan, A.J., Levy, L.M., 2014. Genetics of Alzheimer disease. AJNR Am. J. Neuroradiol. 35, 457–458.

Sarkar, G., Saha, N.R., Roy, I., Bhattacharyya, A., Bose, M., Mishra, R., Rana, D., Bhattacharjee, D., Chattopadhyay, D., 2014. Taro corms mucilage/HPMC based transdermal patch: an efficient device for delivery of diltiazem hydrochloride. Int. J. Biol. Macromol. 66, 158–165.

Suresh, G., Manjunath, K., Venkateswarlu, V., Satyanarayana, V., 2007. Preparation, characterization, and in vitro–in vivo evaluation of lovastatin solid lipid nanoparticles. AAPS Pharm. Sci. Tech. 8, 1–9.

Tiseo, P.J., Foley, K., Friedhoff, L.T., 1998. An evaluation of the pharmacokinetics of donepezil HCl in patients with moderately to severely impaired renal function. Br. J. Clin. Pharmacol. 46, 56–60.

Tiwari, R., Pathak, K., 2011. Nanostructured lipid carrier versus solid lipid nanoparticles of simvastatin: comparative analysis of characteristics, pharmacokinetics and tissue uptake. Int. J. Pharm. 41, 232–243.

Wissing, S.A., Muller, R.H., 2002. Solid lipid nanoparticles as carrier for sunscreens: in vitro release and in vivo skin penetration. J. Control Release 81, 225–233.

Yuxiu, Z., Dongmei, C., Xin, K., Liang, F., 2014. Design and evaluation of a novel transdermal patch containing diclofenac and teriflunomide for rheumatoid arthritis therapy. Asian J. Pharm. Sci. 9, 251–259.

Zhao, X., Yang, C., Yang, K., Li, K., Hu, H., Chen, D., 2010. Preparation and characterization of nanostructured lipid carriers loaded traditional Chinese medicine, zedoary turmeric oil. Drug Dev. Ind. Pharm. 36 (7), 773–780.